A dictionary-matrix separation and Viterbi decoding for Miller code in RFID tag collision

Yu Zeng (yv.zeng@gmail.com)
Yunnan University https://orcid.org/0000-0002-7393-2859
Hongwei Ding
Yunnan University https://orcid.org/0000-0003-0827-5984

Research Article

Keywords: UHF RFID, Viterbi, Miller code, Tag collision, Signal separation

Posted Date: June 10th, 2022

DOI: https://doi.org/10.21203/rs.3.rs-1648443/v1

A dictionary-matrix separation and Viterbi decoding for Miller code in RFID tag collision

Yu Zeng,[1,2] Hongwei Ding[1]
[1] School of Information Science & Engineering, Yunnan University, 650091, China.
[2] School of Electrical & Information Technology, Yunnan Minzu University, 650504, China.
Correspondence should be addressed to Hongwei Ding; hwding@ynu.edu.cn
The 16-digit ORCID of the first author is: 0000-0002-7393-2859
The 16-digit ORCID of the corresponding author is: 0000-0003-0827-5984

Abstract:

With the help of perception technologies such as Radio Frequency Identification (RFID), information interaction will expand from communication devices to various non-communication items in daily life, and the era of ubiquitous personal communication networks may come. In an Ultra High Frequency (UHF) RFID system, however, signal collision often occurs during multiple tags identification. The collision resolution across a Media Access Control (MAC) layer and a physical layer can significantly improve communication efficiency. As a delay code, Miller code is often used in the UHF RFID system. Because its baseband signal has more subcarriers, it has higher anti-noise performance. This paper adopt the cross-layer resolution and proposes a new collision separation and decoding algorithm for the Miller code of the RFID system. This algorithm separates the collision signal by clustering and dictionary matrix firstly, and then decode the separated signal by Viterbi method. In this simulation, we generate a set of simulation data to evaluate the proposed algorithm. The simulation results show that the separation efficiency of the proposed algorithm is about 25% higher than that of traditional methods. Furthermore, we evaluate the performance of the proposed algorithm in this measured data, and obtain 8% higher system throughput than a traditional dynamic ALOHA system.

Key Words: UHF RFID; Viterbi; Miller code; Tag collision; Signal separation

1 Introduction

Personal communication industry has developed rapidly in the past 20 years, and personal mobile communication devices can always be connected to Internet. With the help of perception technologies such as radio frequency identification (RFID) [1] and wireless sensor networks, Internet of Things era [2] will expand information interaction from Internet devices to personal non-communication items in daily life, such as clothes, utensils, and furniture. The interaction is based on personal needs to achieve information acquisition, transmission, storage, decision-making, use and other services between people and people or between people and things, providing individuals with information services and applications anytime and anywhere to realize a ubiquitous personal communication network.

RFID is an automatic identification system that enables tags attached to items to exchange data with a reader via radio waves. Each RFID tag has a unique global identity, so the items entering the network will also be unique. In an RFID system, multiple tags usually need to be identified at the

same time to improve the identification efficiency. Since tags transmit data sharing the same wireless channel, tag collisions are unavoidable. Anti-collision is one of the main techniques to resolve the collision, and is generally performed at the Media Access Control (MAC) layer [3-5]. When the collision occurs, the tag signal has to retransmitted. The retransmission increases with the collision, which will cause a low identification efficiency. A physic-layer separation technique [6] can directly recover the tag signal from the collision signal. The advantage of the technique is to reduce retransmissions and improving the identification efficiency, and thus it has also been used in RFID tag anti-collision in recent years. As a common communication technique, on the other hand, signal coding can effectively resist interference signals [7], and anti-collision is essentially an anti-interference technique. Hence, good coding can improve the anti-collision performance of RFID tags at the physical layer.

Frequency drift is a common phenomenon in wireless communication [8] and also common in Ultra High Frequency (UHF) RFID, which makes traditional matched filters [9] difficult to obtain better decoding results. As one of the most popular UHF RFID standards, EPC C1 Gen2 [10] specifies that the signal can use FM0 and Miller encoding. Since FM0 or Miller decoding make a decision for a symbol by its phase change rather than by its period, the frequency drift can be better solved. Compared with the FM0 code, the Miller code has not only the phase jump but also the subcarrier, which makes the Miller code have better anti-noise performance. However, the existence of subcarriers also makes Miller code more complicated than FM0 code. For the reason, many RFID physical layer anti-collision methods are concentrated in the FM0 code [11-13]. This paper will optimize Miller decoding to improve the anti-collision performance of RFID tags. In traditional Miller code decoding, it removes the subcarrier by bitwise XOR with the clock signal [7, 14-15], and then decode through phase jump. However, the separation of the collision signal at the physical layer will produce separation errors, which will still be there even after the subcarrier removal. Thus, the phase jump is no longer accurate, resulting in an increase in decoding errors.

For that, this paper proposes a maximum likelihood Viterbi decoding method suitable for the physical layer anti-collision, which adopts a dictionary matrix to eliminate separation errors. In experiments, through both of the simulated and measured tag collision data of Miller code, results show that the proposed method has almost no bit errors at 10dB, the separation efficiency can reach 100% at 15dB and the throughput can finally reach 0.55.

2 Signal separation and decoding

MAC-layer collision resolution adopts random multiple access method [3-5]，where each tag selects transmission time slot randomly, and if a collision occurs, the signal will be retransmitted again. However, the MAC-layer method regards the collision time slot as an invalid one. Thus, the communication efficiency is not high. In the physical layer separation method, on the other hand, the signal in the collision time slot can be recovered [6]. Since the method treats the collision time slot as a valid one, the communication efficiency is improved. The collision signal is actually the superposition of several tag signals. Fig. 1(a) shows the collision signals superimposed by two tag signals. Usually, after the binary digital unipolar code with N tags is demodulated by Inphase Quadrature (IQ) [12], there will be $J = 2^N$ clusters when its sampling points are mapped to a complex plane. Each cluster center point is actually a complex number composed of the real and imaginary parts, and can be expressed as [16]

$$0,\ h_1,\ h_2,\ \ldots,\ h_N,\ h_1+h_2,\ h_1+h_3,\ \ldots,\ h_{N-1}+h_N,\ \ldots,\ h_1+h_2+\ldots+h_N \tag{1}$$

where h_1, h_2, … h_N are the complex fading coefficients of each tag, respectively. After clustering, each sampling point can be separated into N source points according to the center point of (1), which is

$$\underbrace{00...0}_{N},\ \underbrace{10...0}_{N},\ \underbrace{01...0}_{N},\ \underbrace{00...1}_{N},\ \underbrace{110...0}_{N},\ \underbrace{1010...0}_{N},\ \ \ldots\ \ \underbrace{0...011}_{N},\ \ldots\underbrace{11...1}_{N} \qquad (2)$$

Through (1) and (2), the collision signals can be separated. Fig. 1(b) shows the case where two tag collision signals are mapped onto a complex plane. Each sampling point is decomposed into 00, 01, 10 or 11when its cluster center point is 0, h_1 ,h_2 or h_1+h_2 .

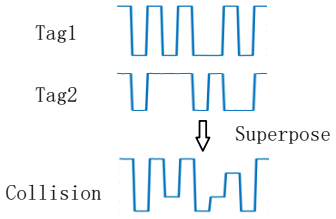

(a) Collision signal

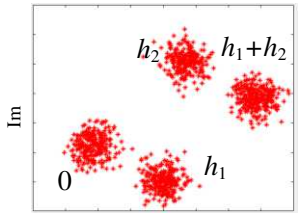

（b） Collision signals mapped to a complex plane

Fig. 1 An example for collision signals separated by a physical layer method

Another physical layer separation method directly decodes each tag signal from the collision signals. For example, FM0 code [11-13] can be viewed as a finite state machine. Using the state machine, Viterbi algorithm [17-18] decoding can quickly find a maximum likelihood path from all search paths to eliminates the interference of other tags, and then use successive interference cancellation to decode each tag one by one.

Except for FM0 code，EPC C1 Gen2[10] also specifies that UHF RFID can adopt Miler code [7, 14-15]. Fig. 2(a) and (b) give the state machine and the signal wave of Miller code, respectively. From the figure, Miller code can be also regarded as a finite state machine diagram like FM0 code [10, 17]. However, each symbol in the Miller code contains a subcarrier, as shown in an example of Fig. 2(c). In the example, the symbol sequence is "010"， and different M represents different subcarrier frequency. The higher the value, the higher the frequency. Conventional Miller decoding first does XOR operation of the coded signal and another square signal with the same subcarrier frequency [14-15] to remove the subcarrier, and then decodes by the phase jump. Fig. 3 shows an example, where M=4 and the decoded symbols are "11".

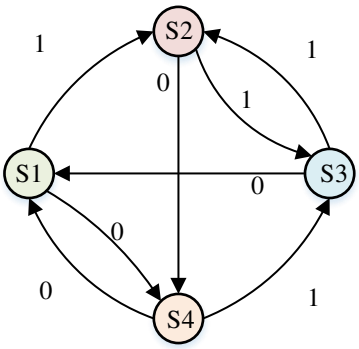

(a) State machine

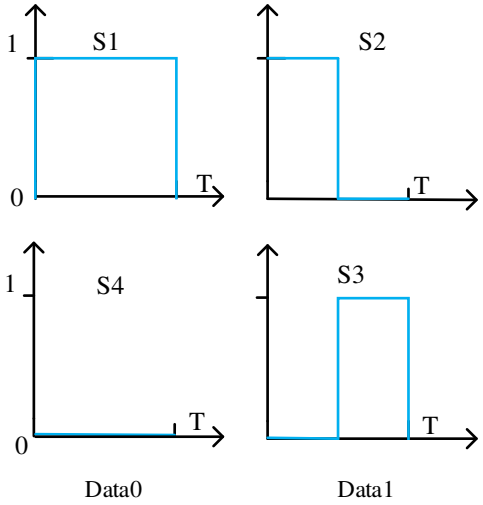

(b) Signal wave of state

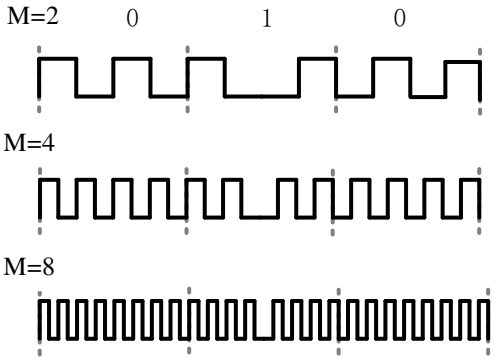

(c) Sub carrier

Figure 2 State machine, signal wave and subcarriers for Miller code

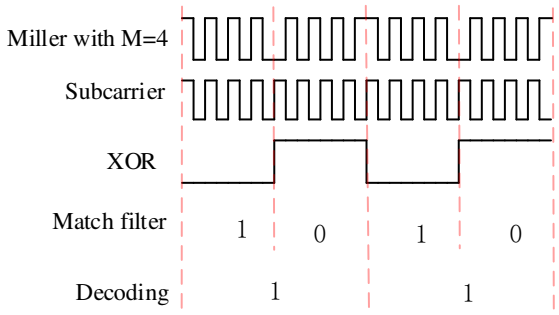

Fig. 3 Conventional Miller decoding

3 Problem description

Collision separation may produce separated noise, as shown in the left of Fig. 4. After the separation, there will be some invalid phase jump, shown in the right of Fig. 4. For Miller code, the jump from the separation noise cannot be eliminated, even after the traditional XOR operation. Since the Miller signals is decoded through the phase jump, the invalid jump will easily produce decoding errors.

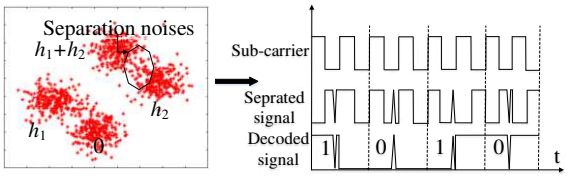

Fig. 4 Subcarrier removal with separation noise in Miller code

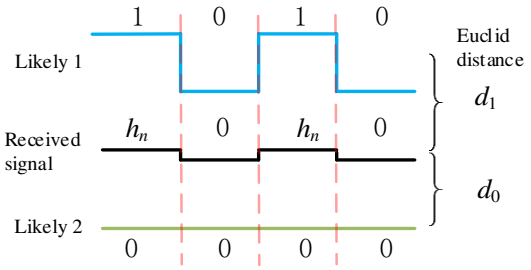

Fig. 5 Finding an incorrect surviving path in the maximum likelihood estimation

In addition, even if the separation error can be canceled, there is still some uncertainty. In the left of Fig. 4, two collision tags form four clusters in a complex plane, where the center of each cluster is marked as 0, h_1, h_2 and h_1+h_2 in clockwise. Since the complex fading coefficient of each tag can not be predicted in advance, the coefficient of its inphase or quadrature part can be large or small, positive or negative. Therefore, the arrangement of the four center points may also be counterclockwise or other order[11]. To determine the position of each center point, a direct method is to estimate the tag fading coefficients. However, either pilot estimation or blind estimation [19-21] will increase the complexity of the system.

Viterbi decoding method [17] does not need to separate the signal first, and can directly recover the tag signal from the collision signal. The method needs to calculate the likelihood distance between observed signals and search signals, and find the maximum likelihood path as a survival

one. However, it also has some problems. Since the signal is a unipolar code, the likely path consists of a normalized 0 or 1. If the fading coefficient of the n-th tag is h_n, its unipolar code signal consists of 0 or h_n, as shown in Fig. 5. If h_n is small, it is easy to misjudge symbol 1 as symbol 0, which leads to an incorrect surviving path.

4 Algorithm

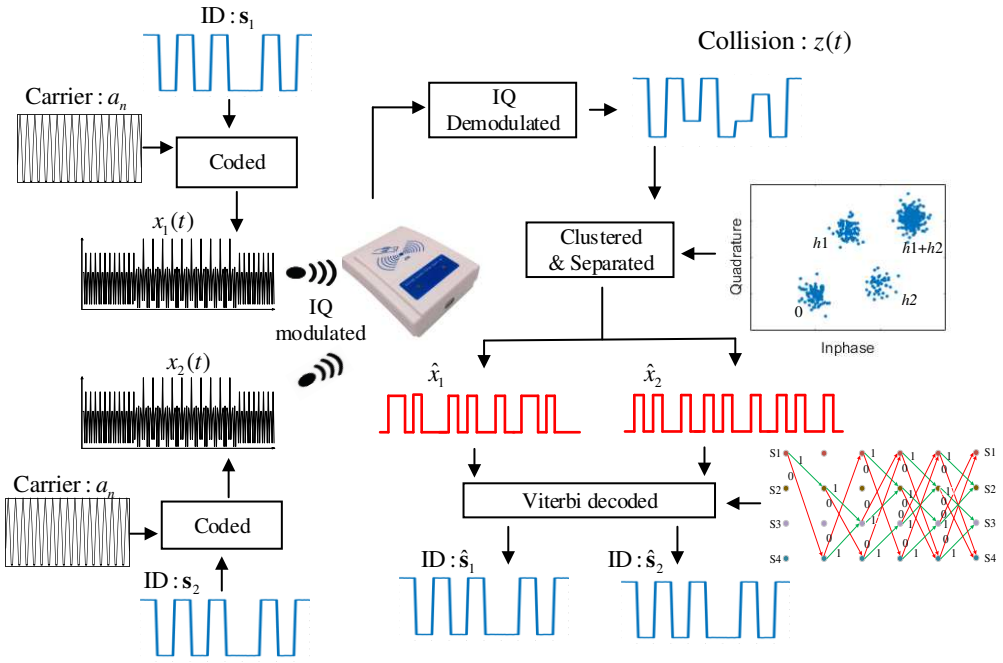

Fig. 6 System flow chart

4.1 System model

In an RFID system, when there are N tags responding in a same time slot, a reader will receive a superimposed signals of the N tags, as shown in Fig. 6. The superimposed signal can be expressed as a complex signal after IQ demodulation, i.e.

$$z(t) = \sum_{n=1}^{N} h_n x_n(t) + \xi(t) + L \tag{3}$$

where

h_n represents a channel attenuation coefficient of the n-th tag, which is usually a time-invariant channel with flat fading[17, 22],

$\xi(t)$ is an additive white Gaussian noise,

L is carrier leakage,

$x_n(t)$ represents the n-th tag signal, denoted as

$$x_n(t) = \sum_{k=1}^{K} e_{k,n} a_n(t - kg_n - b_n) \tag{4}$$

$e_{k,n} \in \{0,1\}^{K\times 1}$ represents the coded sequences from the k'-th symbol $s_{k',n} \in \{0,1\}^{K'\times 1}$ transmitted by the n-th tag,

K is the length of the coded sequences, $K' = K / 2\mathrm{M}$ is the length of the uncoded sequences,

and M is the Miller code order. For example, when M =2, if $s_{k',n}$ is 1, the encoded sequences $e_{4k'+1,n}$, $e_{4k'+2,n}$, $\ldots e_{4(k'+1),n}$ is 1001,

a_n is the modulated pulse waveform,

g_n and b_n represent the symbol period and time delay, respectively.

Fig. 6 shows the basic flow of the proposed algorithm. Firstly, the received signal needs to be sampled, T is denoted as a sampling period, and then the received signal vector $\mathbf{z}=[z_i] \in \mathbb{C}^{1\times I}$ can be obtained after I samplings, where $\mathbb{C}$ is a complex number set and $z_i = z(iT)$, i=1, 2, … I. Next, the separation algorithm is used to obtain N tag signal vectors $\hat{\mathbf{x}}_n$, n=1, 2, … N. Finally, use Viterbi to decode $\hat{\mathbf{x}}_n$ to get the original symbol sequence vector of the n-th tag $\hat{\mathbf{s}}_n=[\hat{s}_{k',n}] \in \{0,1\}^{K'\times 1}$.

4.2 Dictionary separation algorithm

Let $\mathbf{D}=[\mathbf{d}_j] \in \{0,1\}^{J\times N}$ be a dictionary matrix composed of row vectors $\mathbf{d}_j$,where $J=2^N$ and $\mathbf{d}_j \neq \mathbf{d}_n$ when $j \neq n$. Then, the cluster center vector $\mathbf{C}=[c_j] \in \mathbb{C}^{J\times 1}$ can be expressed as

$$\mathbf{C}=\mathbf{DH} \tag{5}$$

where

$c_j \in \mathrm{C}$,

$\mathrm{C}=\{c_{\hat{j}} | \hat{j}=1,2,...J\}$,

$c_{\hat{j}}$ is the cluster center after clustering the collision signal vector ,

$\mathbf{H}=[h_1, h_2, \ldots h_N]^{\mathrm{T}}$.

For the case of two collision tags, the dictionary matrix $\mathbf{D}$ can be expressed as

$$\mathbf{D}=[\mathbf{d}_1^{\mathrm{T}} \quad \mathbf{d}_2^{\mathrm{T}} \quad \mathbf{d}_3^{\mathrm{T}} \quad \mathbf{d}_4^{\mathrm{T}}]^{\mathrm{T}}=\begin{bmatrix} 0 & 1 & 0 & 1 \\ 0 & 0 & 1 & 1 \end{bmatrix}^{\mathrm{T}} \tag{6}$$

There are A_J^J permutations for c_j in the vector $\mathbf{C}$ since the channel coefficient $\mathbf{H}$ is unknown. Even if each cluster center $c_{\hat{j}}$ has been obtained, the cluster center vector $\mathbf{C}$ cannot be determined. Therefor, we need to estimate $\mathbf{C}$.

There is a silent period before a tag transmits its signal [22]. During the time, only the carrier leakage L exists, as shown in Fig. 7. After sampling, the center point c_1' of the cluster can be determined as

$$c_1' = L \rightarrow \mathbf{d}_1 \tag{7}$$

where $\rightarrow$is denoted as a map. In addition, according to EPC Gen2, each tag needs to have the same preamble signal before transmitting RN16 [10] as shown in Fig. 7. Therefore, for the case of two tags, another cluster center point c_4' can be determined as

$$c_4' = h_1 + h_2 + L \rightarrow \mathbf{d}_4 \tag{8}$$

Accordingly, c_1 and c_4 in the vector $\mathbf{C}$ can be estimated by

$$c_1 = \arg\min_{\hat{j}} |c_{\hat{j}} - c_1'| \tag{9}$$

$$c_4 = \arg\min_{\hat{j}} |c_{\hat{j}} - c_4'| \tag{10}$$

respectively. Next, c_2 and c_3 can be determined by the remaining two cluster center points h_1 and h_2. Since the number of collision tags is two, they can also be h_2 and h_1. The two cases above

will produce the same result except the order of separated tag signal is opposite. The mapping is expressed by

$$\{c_2, c_3\} = \mathbf{C} - \{c_1, c_2\} \rightarrow \{\mathbf{d}_2, \mathbf{d}_3\} \tag{11}$$

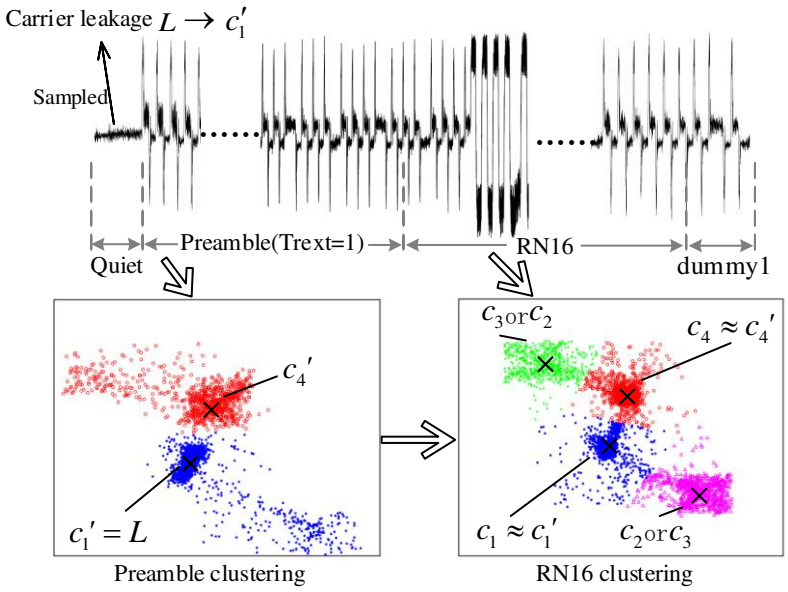

Fig. 7 The determination of relationship between the cluster centers

The vector $\mathbf{C}$ can be determined from (9-11), and then (5) is also determined. Next, from the dictionary matrix $\mathbf{D}$ of (5), the function $\mathbf{f}_{dict}(\cdot)$ between a point in a cluster S_j and $\mathbf{d}_j$ can be written as

$$\mathbf{d}_j = \mathbf{f}_{dict}(z_i), \quad \text{if} \quad z_i \in \mathrm{S}_j \tag{12}$$

where S_j is the cluster with the center c_j. For example, for two tags, if $z_i \in \mathrm{S}_1$, $\mathbf{f}_{dict}(z_i)$ will be [0 0]; if $z_i \in \mathrm{S}_2$, $\mathbf{f}_{dict}(z_i)$ will be [1 0]. Thus, the signal vector $\mathbf{z}$ can be separated form (12) and get a signal matrix $\hat{\mathbf{X}} = [\xi_i] \in \{0,1\}^{I \times N}$ consisting of row vectors ξ_i, where $\xi_i = \mathbf{f}_{dict}(y_i)$. The separation is expressed as

$$\hat{\mathbf{X}} = \mathbf{f}_{sep}(\mathbf{z}) \tag{13}$$

Write the signal matrix $\hat{\mathbf{X}}$ as a matrix consisting of column vector, i.e. $\hat{\mathbf{X}} = [\hat{\mathbf{x}}_n] \in \{0,1\}^{I \times N}$. Therefore, $\hat{\mathbf{x}}_n = [\hat{x}_{i,n}] \in \{0,1\}^{I \times 1}$ is the separated signal of the n-th tag, where $\hat{x}_{i,n} = \hat{x}_n(iT)$ is the i-th sample point.

4.3 Viterbi decoding

Let a likelihood function be

$$p(\hat{\mathbf{x}}_n \,|\, \mathbf{s}_n) \propto -d(\hat{\mathbf{x}}_n, \mathbf{s}_n) \tag{14}$$

where $d(\hat{\mathbf{x}}_n, \mathbf{s}_n)$ represents the Hamming or Euclidean likelihood distance between the n-th tag separated signal $\hat{\mathbf{x}}_n$ and the signal encoded from $\mathbf{s}_n$. Searching a maximum likelihood can decode $\hat{\mathbf{x}}_n$, i.e.

$$\hat{\mathbf{s}}_n = \arg\max_{\mathbf{s}_n} d(\hat{\mathbf{x}}_n, \mathbf{s}_n) \tag{15}$$

For (15), if a brute search is used for $\mathbf{s}_n$, the number of the search is $2^{K'}$, which produces higher computational complexity. Viterbi decoding can be used to reduce the complexity.

Since the symbols $s_{k',n}$, $k'=1, 2, \ldots K'$ are independent of each other, the likelihood distance in (15) can be rewritten as

$$d(\hat{\mathbf{x}}_n, \mathbf{s}_n) = \sum_{k'=1}^{K'} d(\boldsymbol{\chi}_{k',n}, s_{k',n}) \tag{16}$$

where $\boldsymbol{\chi}_{k',n} = [\hat{x}_{k'T'+1,n}, \hat{x}_{k'T'+2,n}, \ldots \hat{x}_{(k'+1)T',n}]$ represents the separated sampling sequence vector of the k'-th symbol, and T' is the number of samples during one symbol period. After (16) substituted into (15), the original search will become a segmented search. Firstly, compare the likelihood distances under the k'-th symbol and save survival paths with smaller likelihood distances. Then, compare the likelihood distances under $k'+1$ symbols until the final symbol. To realize the segmented search, a trellis diagram of the Miller code is given in Fig. 8, where an initial state is S1. Next, from the waveforms of S1-S4 states in Fig. 2(b) and (c) (Fig. 9 gives the waveform of M=4), the likely sequences from $s_{k',n}$ can be generated. Via Fig. 8, Fig. 9 and the Viterbi algorithm, the distance between the likely sequences generated by $\boldsymbol{\chi}_{k',n}$ and $s_{k',n}$ can be calculated step by step. Save the survivor path until the final symbol, and the smallest distance of $\mathbf{s}_n$ will be the decoding result. The algorithm steps are shown in Table 1.

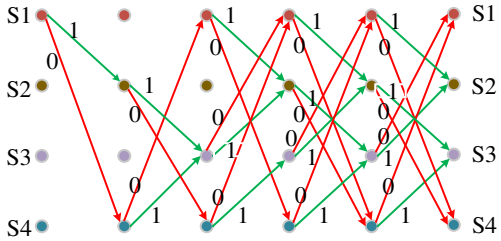

Fig. 8 A trellis diagram of Miller coding

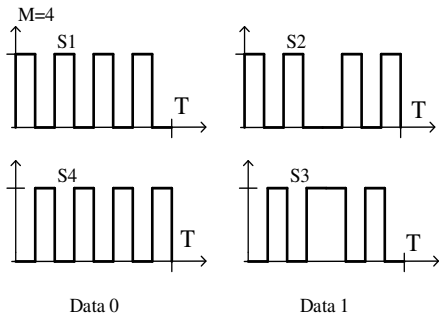

Fig. 9 . Waveforms of states when M=4.

Table 1 Algorithm steps

Input： received signal vector $\mathbf{z}=[z_i] \in \mathbb{R}^{1\times I}$ sampled from $z(t)$
Output： the n-th tag decoded vector $\hat{\mathbf{s}}_n=[\hat{s}_{k',n}] \in \{0,1\}^{K'\times 1}$, $n=1, 2, \ldots N$
Steps： ① Clustering: get the center of each cluster c_j= ② Estimating: get the center vector $\mathbf{C}=[c_j] \in \mathbb{R}^{J\times 1}$ from

(9-11)
③ Dictionary separation: get the separation matrix $\hat{\mathbf{X}} = [\xi_i] \in \{0,1\}^{I \times N}$ from (12-13)
④ Decoding: get each tag decoded signal $\hat{\mathbf{s}}_n = [\hat{s}_{k',n}] \in \{0,1\}^{K \times 1}$ from (16)

5 Experiment setup

In this experiment of the UHF RFID system, One reader will read multiple tags and both the reader and the tags implement the EPC C1 Gen2 standard. The algorithm proposed in this paper will be tested in the RFID system. The experimental data includes simulation data and measured data, as follows.

5.1 Simulation data

The simulated collision signal is generated from (3) and the detailed parameter are shown in Table 2. Since the value of the fading coefficients has a great influence on the performance of the signal decoding, two groups of different fading coefficients are set in the simulated data, shown in Table 3.

Table 2 Parameters in simulated data

Parameters	Description
Link frequency	150kHz
Symbol length K'	16
Baseband sampling frequency	7.5MHz
Symbol Period Tolerance	± 7%
Symbol Delay Tolerance	± 2.46μs
Experiment repetitions	5000
Coding	
Type	Miller
Subcarrier order M	2/4/8
Initial state	S_1
Prefix signal TRext	0

Table 3 Fading coefficient settings

Group	h_1	h_2
1	$0.02\exp(\pi i/3)$	$0.03\exp(\pi i/6)$
2	$0.35\exp(\pi i/3)$	$0.6\exp(\pi i/6)$

5.2 Measured data

The measured data is generated from the UHF RFID system provided by the Radio Frequency Integrated Circuit and System Research Center [23-24] of the School of Information and Communication Engineering, University of Electronic Science and Technology of China. The data is collected by an oscilloscope, and Table 4 shows the detailed parameters in the measured data.

Table 4 Parameters in measured data

Parameters	Description
Antenna	
number	1
type	Right hand circularly polarized antenna
gain	8dBic
Tag-to-reader distance	1m ± 5cm
link frequency	160kHz
Impedance	50Ω

Coding	Miller，M=4
Transmission power	10dBm
Transmit frequency	922.375MHz
Standard	EPC C1 Gen2
Oscilloscope sample rate	50MHz

5.3 Performance evaluation

5.3.1 Algorithms

In order to test the performance of the algorithm proposed in this paper, the simulation compares the performance of the four algorithms, M_Viterbi、F_Viterbi、M_XOR and N_Viterbi, where the fading coefficients are all unknown. M_Viterbi is the algorithm proposed in this paper, which uses Miller code and the conflicting signals are firstly separated and then decoded by Viterbi. F_ Viterbi adopts FM0 code [10] and is decodes by Viterbi after separation [11]. M_Viterbi and F_ Viterbi are compared to analyze different encoding performance with the same decoding. M_XOR adopts Miller code and perform the OR operation [7, 14-15] to decode after separation. M_Viterbi and M_XOR are compared to analyze different decoding performance with the same encoding. N_Viterbi also adopts Miller code[10]，but it directly apply the Viterbi decoding [17] without separation. M_Viterbi and N_ Viterbi are compared to analyze the decoding performance with separation or no separation for the collsion signals. The details of the above algorithms are shown in Table 5.

In the measured data, Miller code uses M=4, and M_Viterbi、M_XOR and N_Viterbi are compared. F_Viterbi is not covered due to its FM0 code.

表 5 Algorithm settings

Algorithm	Encoding	Separation or not	Decoding
M_Viterbi*	Miller	Yes	Viterbi
F_Viterbi	FM0	Yes	Viterbi
M_XOR	Miller	Yes	XOR
N_Viterbi	Miller	No	Viterbi

Note：1. Miller encoding uses M=4

2. K-means clustering is used for the signal separation

3. the algorithm with mark * is the algorithm proposed in this paper

5.3.2 Performance

The following metrics are used to evaluate the performance of the algorithms. The bit error rate (BER) R_e is defined as the ratio of the number of decoded error symbols b_e to the total number of symbols b_t

$$R_e = \frac{b_e}{b_t} \times 100\% \tag{17}$$

Separation efficiency η is defined as the ratio of the number of successfully decoded tags n_s to the total number of tags n_t

$$\eta = \frac{n_s}{n_t} \times 100\% \tag{18}$$

where only when the K' symbols sent by a tag are all successfully decoded, the tag is considered to be successfully decoded. Throughput TPS is defined as the ratio of the average number of

successfully decoded tags L_s in a frame to the length of the frame L_t

$$TPS = \frac{L_s}{L_t} \tag{19}$$

For the above three metrics, the smaller the bit error rate, the higher the separation efficiency and throughput, the better the performance will be.

6 Experiment results

6.1 Simulated data

When signal-to-noise ratio (SNR) is between -25 and 25dB, we give BER, separation efficiency and throughput of the four algorithms under different fading coefficients to compare the performance. The fading coefficients are shown in Table 3, where the fading coefficient in Group 1 is smaller, and that of Group 2 is bigger.

Fig. 10 and 11 show the BER curves. When SNR is -20dB to 5dB, the BER curve of M_Viterbi is always lower than that of F_Viterbi and M_XOR. When SNR is below 10dB, M_Viterbi has no errors. The results show that the performance of M_Viterbi is better than that of F_Viterbi and M_XOR at low SNR. Meanwhile, it can be seen from the comparison of M_Viterbi and F_Viterbi that under the same link frequency, the performance of Miller code is better than that of FM0 code. On the other hand, M_XOR's BER drops significantly when SNR is -5dB to 10dB, which means XOR can reduce errors when the noise is small, but produce more errors when the noise is larger. In Fig. 10，N_Viterbi has a large number of errors ragardless of SNR when the fading coefficient is small. In Fig. 11, N_Viterbi's BER is reduced when the fading coefficient is large, which indicates that the performance of N_Viterbi is related to the fading coefficient.

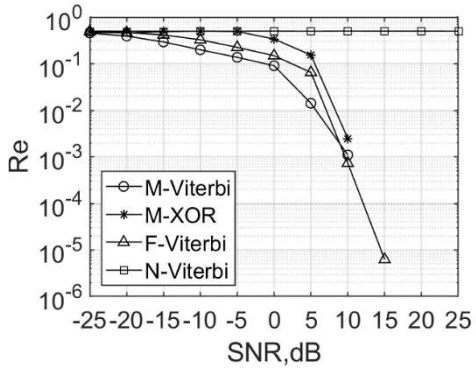

Fig. 10 BER curves under the fading coefficient in Group 1 of Table 3

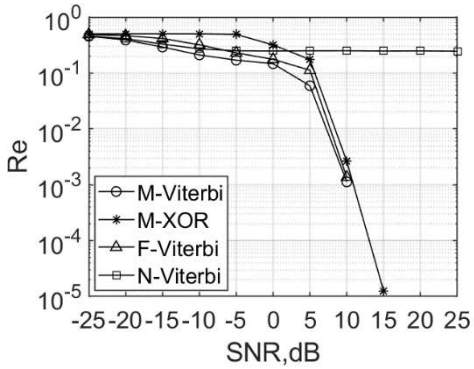

Fig. 11 BER curves under the fading coefficient in Group 2 of Table 3

Fig. 12 and 13 show the separation efficiencies under different fading coefficients, respectively. Similar to the BER curves, the separation efficiency curve of M_Viterbi is always higher than that of F_Viterbi and M_XOR. The separation efficiency of N_Viterbi is related to the fading coefficient. When the fading coefficient is low, Viterbi algorithm will misjudge, as shown in Fig. 12. The separation efficiency of N_Viterbi in Fig. 13 increases with SNR, and tags with a fading coefficient less than 0.5 cannot be decoded correctly, only about 50% decoding efficiency. The reason is consistent with that analyzed in Fig. 5.

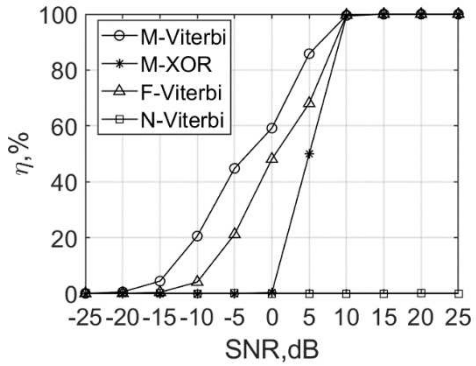

Fig. 12 Separation efficiency under the fading coefficient in Group 1 of Table 3

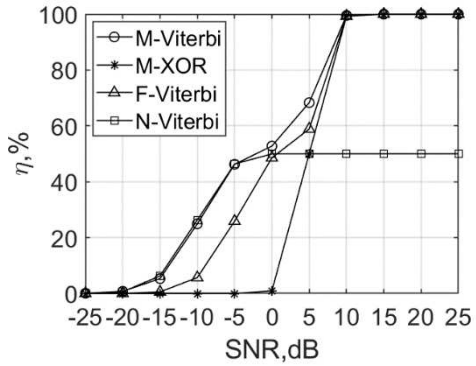

Fig. 13 Separation efficiency under the fading coefficient in Group 2 of Table 3

Fig. 14 and 15 show the throughput of the algorithms applied to an ALOHA system, where a frame length and the number of tags are both set to 128. Firstly, tags select slots randomly. When

two tags collide in a slot, the separation and decoding algorithm is executed. If more than two tags collide, it is considered that they cannot be separated and will be retransmitted in the next frame. In addition, the figures show the pure ALOHA system throughput without separation and decoding, which is close to the theoretical value of 0.367 [25]. It can be seen from the figures that when SNR gradually increases, the throughput of the separation and decoding is greater than that of the pure ALOHA system. The throughput of M_Viterbi, F_Viterbi and M_XOR can eventually reach about 0.55, which shows that the separation and decoding algorithm can increase the throughput of the ALOHA system. When the fading coefficients of the two tags in Fig. 14 are both small, the throughput of the N_Viterbi algorithm is similar to that of the pure ALOHA system, which can only reach 0.367. In Fig. 15, one of tags can be successfully decoded when the fading coefficient is greater than 0.5, so the throughput can reach 0.46.

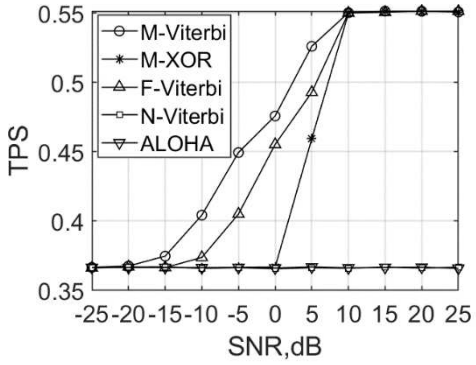

Fig. 14 Throughput under the fading coefficient in Group 1 of Table 3

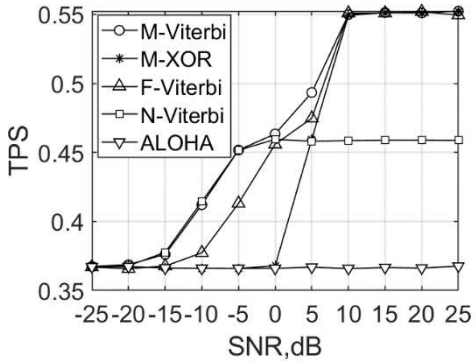

Fig.15 Throughput under the fading coefficient in Group 2 of Table 3

6.2 Measured data

The measurement data in this sub-section includes the data of I channel and Q channel. Fig. 16 shows that of I channel, which shows the preamble and RN16. Since the measured signal is Miller encoded and F_Viterbi is for FM0, only the experimental results of the M_Viterbi, M_XOR and N_Viterbi algorithms are given in Table 6. From the table, M_Viterbi and M_XOR's BERs are both 0, which means M_Viterbi can also perform well for the measured data. Meanwhile, since the measured signal's SNR is low, M_XOR does not generate bit errors. However, N_Viterbi has high requirements on the channel fading coefficient. Thus, it still cannot decode the tag correctly with

only 0.365 throughput even if the noise of the measured data is low, which is close to the theoretical value of the pure ALOHA system throughput..

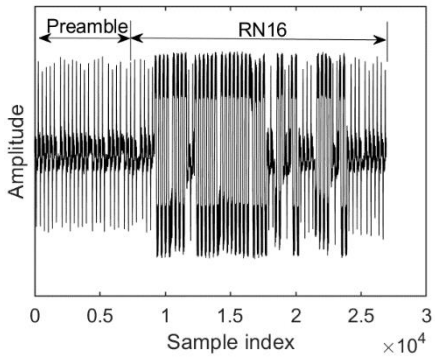

Figure 16 the measured data of I channel

Table6 The performance of the algorithms for the measured data

Metric	M_Viterbi	M_XOR	N_Viterbi
BER	0	0	0.180
Throughput	0.550	0.550	0.365

Note: 1. Three significant digits after the decimal point

7 Conclusions

For a UHF RFID system, this paper uses a physical-layer collision resolution to separate and decode the collision signals in ALOHA random multiple access, to improve the throughput of the system. In this simulation of the ALOHA network, the system throughput reaches 0.55 using the proposed M_Viterbi algorithm when SNR is 10dB. Compared with algorithms of the same decoding algorithm under different encodings, different decoding algorithms under the same encoding, and the same decoding with the same encoding without separation, M_Viterbi algorithm proposed in this paper has better decoding performance. It can also be seen that the Viterbi decoding can also be applied to Miller code, and under the same link frequency, Miller code obtains better decoding performance than FM0 code. When SNR is between -15 and 5dB, the separation efficiency of Viterbi algorithm decoding Miller code is better than that of FM0 code by about 5 dB. On the other hand, the traditional XOR decoding method has more bit errors at lower SNR. When SNR is between -20 and 5dB, the BER and separation efficiency of the algorithm in this paper are better than those of the traditional XOR algorithm 10 to 15 dB. Besides, if the collision signals are not separated, Viterbi algorithm will lead to misjudgment of the surviving path under some fading coefficients. For example, when the channel coefficient is small in this simulation, the throughput of N_Viterbi is not greatly improved compared with pure ALOHA. In addition, this paper also processes the measured UHF RFID collision signals. The experimental results show that the throughput of the proposed algorithm reaches 0.55, which is about 0.2 higher than the traditional ALOHA system.

Since the channel coefficients of three or more collision tags cannot be estimated in this paper, the proposed algorithm only decodes two tags collision. However, in a dynamic frame ALOHA system, the frame length and the number of signal sources can be approximately equal, and the probability of collision of three or more signal sources is relatively small, so the algorithm in this paper can solve most of the collision time slots in the system. It can also be seen from the

experimental results of this paper that the separation for the slot with two collision tags can also further improve the throughput. In addition, in the measured data experiment in this paper, we collect the collision signal received by the reader and let some softwares process the signals further. A more complete test should be to load the algorithm into a reader and evaluate the algorithm performance. Therefore, in the future work, we will load each algorithm into the RFID reader to complete more experimental results.

8 Acknowledgments

Thanks to the Radio Frequency Integrated Circuit and System Research Center of the School of Information and Communication Engineering, University of Electronic Science and Technology of China for providing the RFID system hardware equipment, and thanks to Chu Chu, a doctoral candidate in the research center for helping to collect the data for the experiment.

9 Statements and Declarations

The research and publication of this article was funded by The National Natural Science Foundation of China [62161052, 61461053, 61461054] .

10 Competing Interests

The authors declare that there is no competing interest regarding the publication of this paper.

11 Data Availability

The research data used to support the findings of this study are included within this paper.

12 References

[1] Klaus Finkenzeller. RFID Handbook: Fundamentals and Applications in Contactless Smart Cards, Radio Frequency Identification and Near-Field Communication, Edition 3. John Wiley & Sons, Nov., 2010

[2] Syed A. Ahson, Mohammad Ilyas. RFID Handbook: Applications, Technology, Security, and Privacy. CRC Press,Dec., 2017

[3] Jian Su; Zhengguo Sheng; Liangbo Xie; Gang Li; Alex X. Liu. Fast Splitting-Based Tag Identification Algorithm For Anti-Collision in UHF RFID System, IEEE Transactions on Communications, Volume: 67, Issue: 3,Page(s): 2527 - 2538, March 2019. DOI: 10.1109/TCOMM.2018.2884001

[4] Xiulong Liu; Sheng Chen; Jia Liu; Wenyu Qu; Fengjun Xiao; Alex X. Liu; Jiannong Cao; Jiangchuan Liu. Fast and Accurate Detection of Unknown Tags for RFID Systems – Hash Collisions are Desirable, IEEE/ACM Transactions on Networking, Volume: 28, Issue: 1, Page(s): 126 - 139, Feb. 2020. DOI: 10.1109/TNET.2019.2957239

[5] Su, Jian ; Xu, Ruoyu ; Yu, ShiMing ; Wang, BaoWei; Wang, Jiuru. Idle Slots Skipped Mechanism based Tag Identification Algorithm with Enhanced Collision Detection, KSII Transactions on Internet and Information Systems, Volume 14 Issue 5, Pages.2294-2309,May 2020. DOI: 10.3837/tiis.2020.05.024

[6] Yuxiao Hou; Yuanqing Zheng. PHY-Tree: Physical Layer Tree-Based RFID Identification, IEEE/ACM Transactions on Networking, Volume: 26, Issue: 2, Page(s): 711 - 723, April 2018. DOI: 10.1109/TNET.2018.2791938

[7] Young Gil Kim; A. J. Han Vinck. Anticollision Algorithms for FM0 Code and Miller Subcarrier Sequence in RFID Applications, IEEE Transactions on Vehicular Technology, Volume: 67, Issue: 6, Page(s): 5168 - 5173, June 2018. DOI: 10.1109/TVT.2018.2817587

[8] Li J, Wu H, Zeng Y. Recovery of collided RFID tags with frequency drift on physical layer[J]. IEEE/CAA Journal of Automatica Sinica, Volume: 7, Issue: 6, Page(s): 1593 – 1603, November 2020, DOI: 10.1109/JAS.2019.19117202019.

[9] Bailey J P, Beal A N, Dean R N, et al. A digital matched filter for reverse time chaos[J]. Chaos: An Interdisciplinary Journal of Nonlinear Science, 2016, 26(7): 073108.

[10] EPC radio frequency identity protocols class-1 generation-2 UHF RFID protocol for communications at 860 MHz-960 MHz[S]. November, 2013.

[11] Haifeng Wu; Xiaogang Wu; Yi Li; Yu Zeng. Collision Resolution With FM0 Signal Separation for Short-Range Random Multi-Access Wireless Network, IEEE Transactions on Signal and Information Processing over Networks, Volume: 7, Page(s): 438 - 450, June 2021. DOI: 10.1109/TSIPN.2021.3093000

[12] Aggelos Bletsas; John Kimionis; Antonis G. Dimitriou; George N. Karystinos. Single-Antenna Coherent Detection of Collided FM0 RFID Signals, IEEE Transactions on Communications, Volume: 60, Issue: 3,Page(s): 756 - 766, March 2012. DOI: 10.1109/TCOMM.2011.020612.110212

[13] Hamed Salah; Joerg Robert; Hazem A. Ahmed; Khalid Mahmoud; Albert Heuberger. Theoretical Performance Evaluation of UHF-RFID Systems With Multi-Antenna Maximum-Likelihood Decoding, IEEE Journal of Radio Frequency Identification, Volume: 3, Issue: 2, Page(s): 108 - 117, June 2019. DOI: 10.1109/JRFID.2019.2909504

[14] Xuanxuan Lu , Jing Li. New Miller Codes for Run-Length Control in Visible Light Communications[J]. IEEE Transactions on Wireless Communications,2018, 17(3), 1798–1810.

[15] Yu Zeng, Hongwei Ding, "A Physical-Layer UHF RFID Tag Collision Resolution Based on Miller Code", Wireless Communications and Mobile Computing, vol. 2021, Article ID 6636846, 11 pages, 2021. DOI: 10.1155/2021/6636846

[16] Shen D, Woo G, Reed D P, et al. Separation of multiple passive RFID signals using software defined radio[C]//2009 IEEE International Conference on RFID. IEEE, 2009: 139-146.

[17] K. Fyhn, R. M. Jacobsen, P. Popovski, A. Scaglione and T. Larsen, "Multipacket Reception of Passive UHF RFID Tags: A Communication Theoretic Approach," in IEEE Transactions on Signal Processing, vol. 59, no. 9, pp. 4225-4237, Sept. 2011, doi: 10.1109/TSP.2011.2159499.

[18] Scherhäufl M, Rudić B, Stelzer A, et al. A blind calibration method for phase-of-arrival-based localization of passive UHF RFID transponders[J]. IEEE Transactions on Instrumentation and Measurement, 2018, 68(1): 261-268.

[19] Fuhrwerk M, Moghaddamnia S, Peissig J. Scattered pilot-based channel estimation for channel adaptive FBMC-OQAM systems[J]. IEEE Transactions on Wireless Communications, 2017, 16(3): 1687-1702.

[20] Choi J M, Oh Y, Lee H, et al. Pilot-aided channel estimation utilizing intrinsic interference for FBMC/OQAM systems[J]. IEEE Transactions on Broadcasting, 2017, 63(4): 644-655.

[21] Mezghani A, Swindlehurst A L. Blind estimation of sparse broadband massive MIMO channels with ideal and one-bit ADCs[J]. IEEE Transactions on Signal Processing, 2018, 66(11): 2972-2983.

[22] Angerer C, Langwieser R, Rupp M. RFID reader receivers for physical layer collision recovery[J]. IEEE Transactions on Communications, 2010, 58(12): 3526-3537.

[22] Jung S C, Kim M S, Yang Y. A reconfigurable carrier leakage canceler for UHF RFID reader front-ends[J]. IEEE Transactions on Circuits and Systems I: Regular Papers, 2010, 58(1): 70-76.

[23] Wen Guangjun, et al. Technique & Design in Wireless Communication Radio Circuit. Beijing: Electronics industry Press, 2010

[24] Centre for RFIC and System Technology in University of Electronic Science and Technology in China. https://faculty.uestc.edu.cn/shepinjichengdianluyuxitongyanjiuzhongxin/en/index.htm

[25] Wu H F, Zeng Y, Feng J H. Binary tree slotted aloha for passive RFID tag anti-collision[J]. IEEE Trans. Parallel and Distributed Syst-ems, 2013, 24(1): 19-31.